Nepmucin, a novel HEV sialomucin, mediates L-selectin–dependent lymphocyte rolling and promotes lymphocyte adhesion under flow

Eiji Umemoto,[1] Toshiyuki Tanaka,[1] Hidenobu Kanda,[1] Soojung Jin,[1] Kazuo Tohya,[3] Kazuhiro Otani,[1] Takahiro Matsutani,[1] Masanori Matsumoto,[1,2] Yukihiko Ebisuno,[1] Myoung Ho Jang,[1] Minoru Fukuda,[4] Takako Hirata,[2] and Masayuki Miyasaka[1]

[1]Laboratory of Immunodynamics, Department of Microbiology and Immunology, Graduate School of Medicine and [2]The 21st Century Center of Excellence Program, Research Institute for Microbial Diseases, Osaka University, Osaka 565-0871, Japan
[3]Department of Anatomy, Kansai College of Oriental Medicine, Osaka 590-0482, Japan
[4]Glycobiology Program, Cancer Research Center, The Burnham Institute, La Jolla, CA 92037

Lymphocyte trafficking to lymph nodes (LNs) is initiated by the interaction between lymphocyte L-selectin and certain sialomucins, collectively termed peripheral node addressin (PNAd), carrying specific carbohydrates expressed by LN high endothelial venules (HEVs). Here, we identified a novel HEV-associated sialomucin, nepmucin (mucin not expressed in Peyer's patches [PPs]), that is expressed in LN HEVs but not detectable in PP HEVs at the protein level. Unlike conventional sialomucins, nepmucin contains a single V-type immunoglobulin (Ig) domain and a mucin-like domain. Using materials affinity-purified from LN lysates with soluble L-selectin, we found that two higher molecular weight species of nepmucin (75 and 95 kD) were decorated with oligosaccharides that bind L-selectin as well as an HEV-specific MECA-79 monoclonal antibody. Electron microscopic analysis showed that nepmucin accumulates in the extended luminal microvillus processes of LN HEVs. Upon appropriate glycosylation, nepmucin supported lymphocyte rolling via its mucin-like domain under physiological flow conditions. Furthermore, unlike most other sialomucins, nepmucin bound lymphocytes via its Ig domain, apparently independently of lymphocyte function–associated antigen 1 and very late antigen 4, and promoted shear-resistant lymphocyte binding in combination with intercellular adhesion molecule 1. Collectively, these results suggest that nepmucin may serve as a dual-functioning PNAd in LN HEVs, mediating both lymphocyte rolling and binding via different functional domains.

CORRESPONDENCE
Toshiyuki Tanaka:
tanaka@orgctl.med.osaka-u.ac.jp

Abbreviations used: C1GnT, core1 extension-β1,3-*N*-acetylglucosaminyltransferase; C2GnT, core2 β-1,6-*N*-acetylglucosaminyltransferase; FucTVII, α-1,3-fucosyltransferase VII; GlyCAM-1, glycosylation-dependent cell adhesion molecule 1; HEV, high endothelial venule; ICAM-1, intercellular adhesion molecule 1; LSST, L-selectin ligand sulfotransferase; MAdCAM-1, mucosal addressin cell adhesion molecule 1; OSGE, *O*-sialoglycoprotein endopeptidase; PNAd, peripheral node addressin; PP, Peyer's patch; VLA-4, very late antigen 4.

The trafficking of lymphocytes from the blood into LNs and Peyer's patches (PPs) is mediated by a cascade of adhesive interactions between circulating lymphocytes and the specialized endothelial cells of high endothelial venules (HEVs) (1, 2). The adhesive interactions include rolling, firm adhesion, and transendothelial migration of lymphocytes across the HEV wall. In particular, lymphocyte rolling on the luminal surface of LN HEVs is governed by the interaction of lymphocyte L-selectin with specific carbohydrate determinants presented on certain sialomucins expressed by LN HEVs (3).

The online version of this article contains supplemental material.

L-selectin, a C-type lectin cell adhesion molecule, specifically recognizes a capping group of *O*-glycans known as 6-sulfo sialyl Lewis x in which the C-6 position of GlcNAc within the sialyl Lewis x is modified with sulfate (3). This structure can be presented at both core-2 branches and extended core-1 structures of the *O*-glycans of HEV-associated sialomucins and shows L-selectin ligand activities in both positions (4). Genetic studies in mice demonstrated that certain patterns of fucosylation and carbohydrate sulfation are indeed required for L-selectin ligand functions in LN HEVs and that α-1,3-fucosyltransferase VII (FucTVII) (5) and L-selectin ligand sulfotransferase (LSST, also

known as HEC GlcNAc-6-sulfotransferase) (6, 7) are principal enzymes for the biosynthesis of 6-sulfo sialyl Lewis x in LN HEVs. This structure is recognized by an HEV-specific mAb MECA-79 (8) that effectively blocks lymphocyte rolling on LN HEVs (9). The function-blocking activity of the MECA-79 mAb is explained by an overlap of its recognition epitope, an extended core-1 structure modified with GlcNAc-6-sulfate, with the L-selectin recognition determinant (4). Accordingly, the MECA-79 mAb and L-selectin recognize essentially the same glycoprotein complex in LN HEVs. These glycoproteins are collectively termed peripheral node addressin (PNAd).

Soluble L-selectin chimeric proteins and MECA-79 mAb have permitted the biochemical identification of the PNAds of mouse peripheral LNs and human tonsils as a series of heterogeneous glycoproteins. Some of these have been cloned. These molecules include glycosylation-dependent cell adhesion molecule 1 (GlyCAM-1) (10), CD34 (11, 12), endomucin (13, 14), and podocalyxin (15). Of these, CD34, endomucin, and podocalyxin are broadly distributed in vascular endothelial cells in various organs, but L-selectin–reactive glycoforms of these sialomucins are seen in LN HEVs only, demonstrating the importance of tissue-specific post-translational glycosylation events in LN HEVs for the generation of functional PNAd. Additional MECA-79–reactive glycoproteins of 75, 115, and 200 kD have been reported in mouse peripheral LNs (16, 17), but their molecular nature remains to be determined.

Although PNAd expressed by LN HEVs is critical for lymphocyte rolling on LN HEVs, the mucosal addressin cell adhesion molecule 1 (MAdCAM-1) plays a vital role for both lymphocyte rolling on and adhesion to PP HEVs (17–19). MAdCAM-1 is a sialomucin-type cell adhesion molecule and carries a mucin-like domain and three (rodent) or two (human) Ig domains in its extracellular region (20, 21). The first Ig domain of MAdCAM-1 directly interacts with $\alpha 4\beta 7$ integrin (22), mediating both lymphocyte rolling on and firm adhesion to PP HEVs. In addition, MAdCAM-1 expressed in mesenteric LN HEVs is decorated with L-selectin–reactive sugar chains and supports L-selectin–dependent lymphocyte rolling (17). Thus, the mucosal addressin MAdCAM-1 may contribute to mucosal tissue–specific lymphocyte trafficking by bridging the rolling and adhesion steps of lymphocytes in PP HEVs. On the other hand, no PNAd component that can mediate both the rolling and adhesion steps of lymphocytes in LN HEVs has yet been identified.

In this study, we identified a novel sialomucin, nepmucin (mucin not expressed in PPs), which is expressed in LN HEVs but not detectable in PP HEVs at the protein level. Nepmucin carries a mucin-like domain and a single V-type Ig domain. We show that certain isoforms of nepmucin (75 and 95 kD) expressed in LN HEVs carry MECA-79 epitopes and bind L-selectin. Nepmucin that has been appropriately modified with L-selectin–reactive sugar chains supports L-selectin–dependent lymphocyte rolling through its mucin-like domain in vitro. In addition, nepmucin mediates lymphocyte binding through its Ig domain, and this binding appears to be independent of the LFA-1 or very late antigen 4 (VLA-4) adhesion pathway. Under physiological flow conditions, in combination with intercellular adhesion molecule 1 (ICAM-1), nepmucin promotes chemokine-driven, shear-resistant lymphocyte binding. These observations suggest that the novel LN HEV-associated sialomucin nepmucin can serve as a dual-functioning PNAd component, regulating both the rolling and adhesion steps of lymphocytes in LN HEVs.

RESULTS

Molecular cloning of cDNA encoding nepmucin

In a search for novel HEV-associated molecules by gene expression profiling (23, 24), we identified a cDNA fragment (GS11753) that is preferentially expressed in PNAd$^+$ HEVs. By screening a cDNA library prepared from PNAd$^+$ HEVs, we obtained several full-length cDNA clones encoding a type I

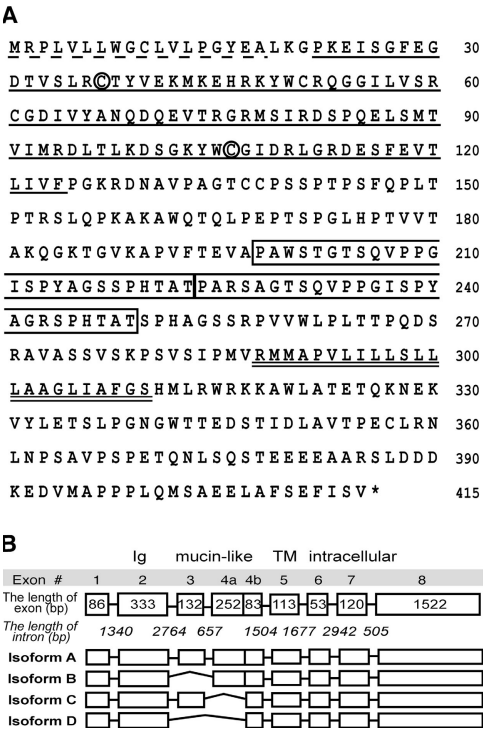

Figure 1. Amino acid sequence of mouse nepmucin and putative exon/intron structure. (A) The deduced amino acid sequence of nepmucin. The putative signal sequence and the transmembrane region are represented by a broken underline and double underline, respectively. The putative Ig domain is underlined, and the cysteine residues participating in the Ig domain structure are circled. The tandem repeats in the mucin-like domain are boxed. (B) The exon/intron structure of mouse nepmucin gene and splicing isoforms. The genomic structure of nepmucin was deduced by comparing the genomic sequence (AL591145) with the cDNA sequence of each nepmucin isoform (isoforms A, B, C, and D). All intron-exon boundaries follow the AG/GT rules. The nucleotide sequences of the nepmucin isoforms have been submitted under accession numbers AB243063, AB243064, AB243065, and AB243066. TM, transmembrane domain.

transmembrane protein of 415 amino acids (Fig. 1 A). The identified start codon is followed by a hydrophobic signal peptide, a single V-type Ig domain, and a mucin-like domain. The Ig domain shows substantial identity at the amino acid level to the corresponding region of human CMRF-35A (25) (40%), CMRF-35H (26) (38%), mouse DIgR (27) (40%), and mouse polymeric Ig receptor (28) (34% with V1 Ig domain). The mucin-like domain (43% serine, threonine, and proline residues) possesses tandem repeats of 26 amino acid residues, a pattern that is often observed in classical mucins (29), and is predicted to be heavily *O*-glycosylated. No *N*-linked glycosylation site (N-X-S/T) was observed. The cytoplasmic tail contains a single potential protein kinase C phosphorylation site (S/T-X-R/K) and a negatively charged amino acid stretch at the COOH terminus. We assigned the name nepmucin (mucin not expressed in PPs) to this molecule because of its structural characteristics and selective expression in LN HEVs as described below. Comparison of the isolated cDNA sequences with the corresponding genomic sequence (AL591145) showed that the nepmucin gene is comprised of eight exons that undergo alternative splicing to generate four isoforms (isoforms A–D, Fig. 1 B). The mouse nepmucin gene is located on chromosome 11 and one nepmucin isoform (isoform D) has been reported as CLM-9 without known functions (30). The differentially spliced exons (exons 3 and 4a) encode the mucin-like domain, and thus each nepmucin isoform has a mucin-like domain of a different size.

Cellular and tissue distribution of nepmucin

We next examined nepmucin mRNA expression in various types of cells by RT-PCR. Nepmucin mRNA could be detected in the PNAd$^+$ HEVs and MAdCAM-1$^+$ HEVs, but not in any of the cultured endothelial cell lines examined (Fig. 2 A). Nepmucin mRNA expression was also observed in some myeloid lineage cell lines (WEHI3B, MH-S, and P388D1) and CD11c$^+$ DCs, but not in a mast cell line (P815) or purified T and B lymphocytes. The expression of nepmucin in DCs was detected in the CD11b$^+$CD8$^-$ subset but not the CD11b$^-$CD8$^+$ subset (unpublished data). These results indicate that nepmucin is preferentially expressed in certain types of endothelial and myeloid lineage cells. As shown in Fig. 2 B, RT-PCR analysis using a primer pair that can detect all the nepmucin isoforms revealed that splicing isoforms A, B, C, and D (highest expression level) are all expressed in MAdCAM-1$^+$ HEVs at the mRNA level.

To analyze nepmucin expression at the protein level, we performed Western blotting analysis of various tissue samples using an anti-nepmucin mAb (ZAQ2). We found that nepmucin is expressed as multiple bands with approximate molecular sizes of 95, 75, 50, and 35 kD in the stromal cell fraction of peripheral LNs and whole peripheral LN lysates (Fig. 2 C). A similar set of bands, of 80, 70, 50, and 35 kD, was detected in various tissues, including mesenteric LNs, spleen, thymus, lung, heart (highest expression), and kidney. The difference in molecular weight of the antigenic components between peripheral LNs (95 and 75 kD) and other

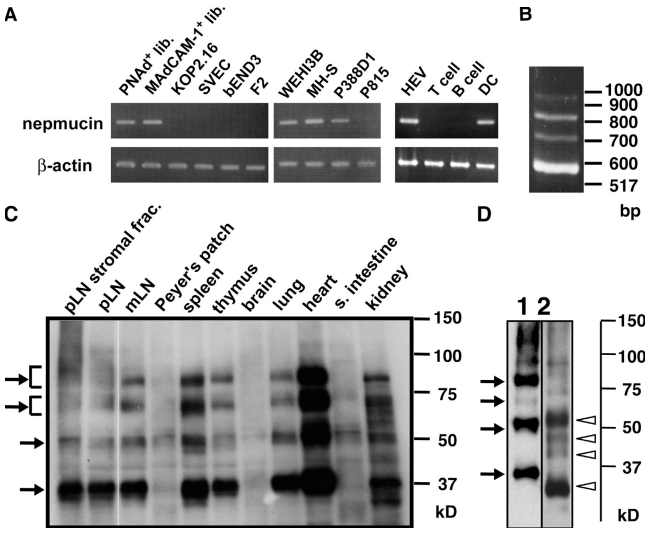

Figure 2. Cell and tissue expression of nepmucin. (A) Nepmucin mRNA expression analyzed by RT-PCR. Left: HEV cDNA libraries (PNAd$^+$ HEVs and MAdCAM-1$^+$ HEVs), endothelial cell lines (KOP2.16, SVEC4-10, bEND3, and F2), monocyte/macrophage cell lines (WEHI3B, MH-S, and P388D1), and a mast cell line (P815) were analyzed. Right: Freshly isolated MAdCAM-1$^+$ HEV cells, T cells, B cells, and DCs were analyzed. The PCR primers were designed to detect all the nepmucin isoforms as a single band. (B) Expression of nepmucin splicing isoforms in freshly isolated MAdCAM-1$^+$ HEVs. A primer pair designed to detect nepmucin isoforms with different product sizes was used. (C) Tissue distribution of nepmucin. The expression of nepmucin was analyzed by Western blotting using the anti-nepmucin mAb ZAQ2, which recognized all four nepmucin variants (arrows). Control rat IgG2a did not give any specific signals (unpublished data). (D) Enzymatic *O*-deglycosylation of nepmucin. Lysates from mouse heart were subjected to immunoprecipitation with ZAQ2 and mock-treated (lane 1) or treated with *O*-glycanase (lane 2). The proteins were analyzed with the anti-nepmucin mAb, ZAQ3. The arrows and arrowheads indicate the four kinds of antigenic components.

tissues (80 and 70 kD) was due to the degree of glycosylation, as described below. Nepmucin was almost undetectable in the small intestine, brain, and PPs. When the *O*-glycan chains of nepmucin were removed enzymatically, the apparent molecular sizes of the nepmucin isoforms decreased markedly (Fig. 2 D, arrows) to 52, 46, 40, and 32 kD (Fig. 2 D, arrowheads), which are in accord with the theoretical molecular sizes of nepmucin isoforms A, B, C, and D, respectively (45, 40, 37, and 32 kD). These observations indicate that nepmucin is expressed in a variety of tissues at the protein level and is heavily modified with *O*-linked carbohydrates. The four nepmucin components detected by Western blotting appeared to represent the nepmucin isoforms A, B, C, and D.

Nepmucin is expressed in HEVs in peripheral and mesenteric LNs, but not in those of PPs

We next performed a histochemical analysis of nepmucin expression in lymphoid and nonlymphoid tissues. As shown in Fig. 3 (A–F), two-color immunofluorescence staining with an anti-nepmucin mAb and HEV-specific mAbs revealed

that nepmucin was expressed in the PNAd$^+$ HEVs and MAdCAM-1$^+$ HEVs of LNs. A small fraction of high endothelial cells appeared to express nepmucin at only low levels (Fig. 3, A–F). Nepmucin was also expressed in small non–HEV-type blood vessels in LNs (unpublished data). Interestingly, nepmucin was not detectable in the blood vessels in PPs, including the MAdCAM-1$^+$ HEVs, at the protein level (Fig. 3, G–I, and Fig. S1, which is available at http://www.jem.org/cgi/content/full/jem.20052543/DC1). No nepmucin signal was observed in PP HEVs by in situ hybridization analysis (Fig. S1 A), whereas low-grade mRNA expression was detected in purified PP HEVs (Fig. S1, B and C). In the spleen, nepmucin was observed in the CD31$^+$ cells in the trabecula and marginal sinus, but not in the CD31$^+$ cells of the central arteriole (Fig. 3, J and K). Nepmucin was also found on the splenic marginal sinus-lining cells known to express MAdCAM-1 (Fig. 3 L) (31). In the heart, nepmucin expression was detected in the intramuscular capillaries but not the arteries (Fig. 3, M–O). These findings demonstrate that nepmucin is selectively expressed in endothelial cells of certain small blood vessels, including the HEVs in peripheral LNs and mesenteric LNs, but not in PPs at the protein level.

Nepmucin in peripheral LN HEVs binds L-selectin and displays the MECA-79 epitope

Because nepmucin has a mucin-like domain and is heavily decorated with *O*-glycans, we hypothesized that HEV-derived nepmucin binds L-selectin and displays the MECA-79 epitope. To test this hypothesis, L-selectin–binding materials purified from peripheral LNs were subjected to Western blotting with the anti-nepmucin mAb. As shown in Fig. 4 A (right, arrowheads), the two major L-selectin–binding molecular species (95 and 75 kD) were detected among the four nepmucin isoforms in total peripheral LN lysates (left, arrows).

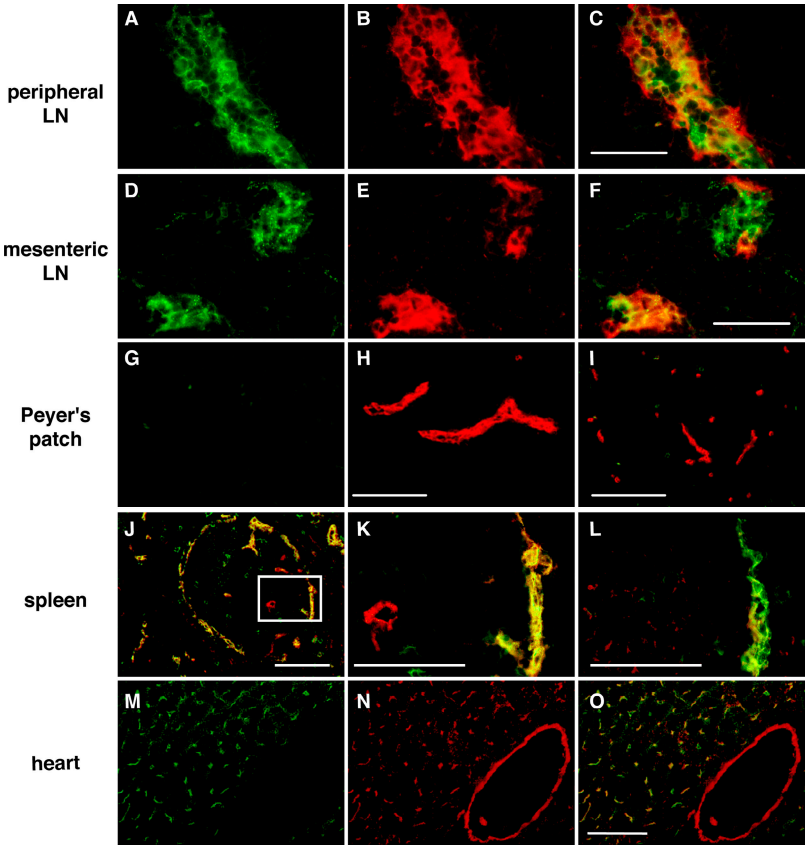

Figure 3. Distribution pattern of nepmucin in mouse tissues. Two-color immunostaining of peripheral LNs with anti-nepmucin (A), anti-PNAd (B), and the merged image (C); two-color immunostaining of mesenteric LNs with anti-nepmucin (D), anti-MAdCAM-1 (E), and the merged image (F). A–F shows that nepmucin was expressed in HEVs in peripheral LNs and mesenteric LNs. Two-color staining of PPs with anti-nepmucin (G) and anti–MAdCAM-1 (H) revealed that nepmucin was undetectable in PP HEVs. Double staining with anti-nepmucin and anti-CD31 showed that nepmucin was also undetectable in non–HEV-type vessels in PPs (I). Two color staining of spleen with anti-nepmucin (J–L) and anti-CD31 (J and K) or anti–MAdCAM-1 (L). The expression of nepmucin was found in the marginal sinus and trabecula (J), but not in central arteries (K). Nepmucin was also detected in the MAdCAM-1$^+$ sinus-lining cells (L). Two-color staining of heart with anti-nepmucin (M), anti-CD31 (N), and the merged image (O) showed that nepmucin was selectively expressed in the intramuscular capillaries but not the arteries. Scale bar, 50 μm (C, F, K, L, and O) and 100 μm (H, I, and J). Negative control rat IgG for anti-nepmucin did not bind tissue sections (unpublished data).

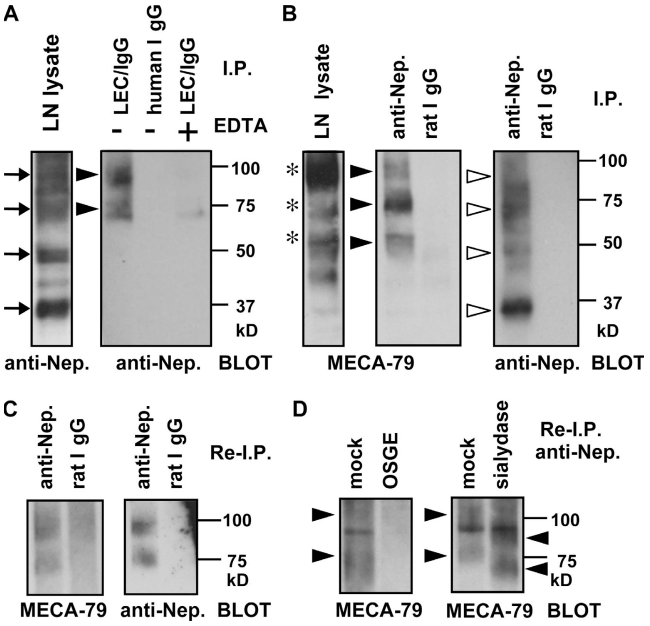

Figure 4. Interaction of nepmucin expressed in peripheral LN HEVs with L-selectin and MECA-79 mAb. (A) Reactivity of L-selectin–binding materials with anti-nepmucin mAb. Total cell lysates of peripheral LNs were immunoblotted with the anti-nepmucin mAb ZAQ2 (left). Lysates of peripheral LNs were precipitated with LEC/IgG chimeric protein or control human IgG, with or without EDTA, and analyzed by Western blotting with ZAQ2 (right). The two major antigenic components are indicated by arrowheads. (B) Reactivity of the nepmucin in peripheral LN HEVs with the MECA-79 mAb. Total cell lysates of peripheral LNs were immunoblotted with the MECA-79 mAb (left). Lysates of mouse peripheral LNs were immunoprecipitated with anti-nepmucin or control rat IgG, and immunoblotted with MECA-79 (middle) or the anti-nepmucin mAb ZAQ2 (right). MECA-79 recognized three nepmucin species (arrows) among the four isoforms (white arrowheads). In A and B, isotype-matched controls to anti-nepmucin and MECA-79 gave no specific signals (unpublished data). (C) Reprecipitation of nepmucin from L-selectin–binding materials. L-selectin–binding materials were reprecipitated with ZAQ2 or rat IgG and analyzed by Western blotting using MECA-79 (left) or ZAQ2 (right). (D) Sensitivity of nepmucin to OSGE or sialydase. L-selectin–binding materials treated with OSGE were subjected to immunoprecipitation with the anti-nepmucin mAb, ZAQ2 (left). Alternatively, L-selectin–binding materials were reprecipitated with ZAQ2 and then treated with sialydase (right). The precipitates were analyzed with MECA-79. Arrowheads indicate the higher molecular weight species of nepmucin.

The addition of EDTA abrogated the precipitation of nepmucin by soluble L-selectin, indicating that the interaction of L-selectin with nepmucin is calcium dependent. When nepmucin was affinity purified from the peripheral LN lysates and subjected to Western blotting with the MECA-79 mAb, at least three nepmucin species (95, 75, and 50 kD) were recognized by the MECA-79 mAb (Fig. 4 B, middle, arrowheads). PNAd components with similar molecular sizes (95, 75, and 50 kD) were detected by the MECA-79 mAb in the total peripheral LN lysates (Fig. 4 B, left, asterisks). As shown in Fig. 4 C, the higher molecular weight species of nepmucin (95 and 75 kD) that were reprecipitated from L-selectin–binding materials were recognized by the MECA-79 mAb. Upon treatment with *O*-sialoglycoprotein endopeptidase (OSGE), which specifically cleaves the peptide backbone of sialomucins (32), the L-selectin–binding materials were no longer precipitated by the anti-nepmucin mAb (Fig. 4 D, left), and upon treatment with sialydase, the 95- and 75-kD nepmucin isoforms showed increased electrophoretic mobilities (Fig. 4 D, right). Collectively, these observations indicate that at least two of the higher molecular weight species of nepmucin that are expressed in peripheral LN HEVs (95 and 75 kD) are decorated with sialylated *O*–linked sugar chains carrying the MECA-79 epitope and bind L-selectin.

Nepmucin is expressed on the luminal surface of LN HEV cells

We next performed immunoelectron microscopic analysis to examine the ultrastructural localization of nepmucin in LN HEVs. As shown in Fig. 5 A, an anti-nepmucin mAb (ZAQ5) bound to the luminal surface of LN HEVs. In particular, the immunoreactivity was mainly in the extended luminal

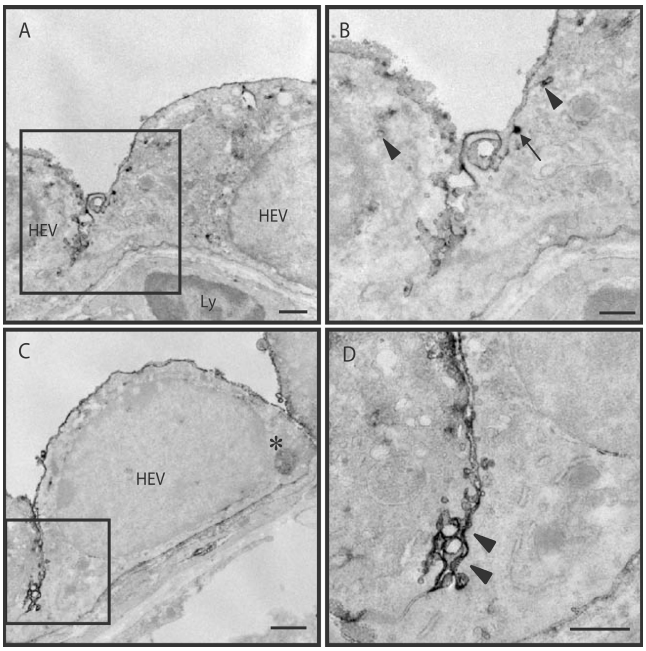

Figure 5. Ultrastructural localization of nepmucin in peripheral LN HEVs. (A) Anti-nepmucin mAb ZAQ5 bound to the vascular luminal surface of LN HEVs. (B) A higher magnification view of the area shown within the square in A shows that nepmucin was frequently concentrated on the extended luminal microvillous process near the intracellular junction. In addition, nepmucin appeared to be localized in the site of internalized plasma membrane (arrow) and in the tubular- or spherical-shaped endosomal vesicles (arrowheads) below the endothelial cell surface. (C) Nepmucin was detectable on the lateral surface of LN HEVs. A multivesicular body (asterisk) was positive for nepmucin. (D) A higher magnification view of the lateral junction area shown within the square in C showed the anti-nepmucin mAb located on the lateral membranes of the high endothelial cells, where they formed loose connections (arrowheads). Ly, lymphocyte. Bars, 1 μm (A and C) and 0.5 μm (B and D).

microvillous processes near the intracellular junctions (Fig. 5 B) where L-selectin–binding substrates reportedly are concentrated (33). As shown in Fig. 5 (C and D), the anti-nepmucin mAb also labeled the lateral surface of HEVs, especially where the endothelial cells form loose connections or are interdigitated (Fig. 5 D), whereas in the basal region, there was little anti-nepmucin mAb immunoreactivity. In addition, the anti-nepmucin mAb appeared to react with the site of internalized plasma membrane (Fig. 5 B, arrow), tubular- or spherical-shaped endosomal vesicles (Fig. 5 B, arrowheads) with the size of 100 to 200 nm, as well as the multivesicular bodies (Fig. 5 C, asterisk) (34). These observations indicate that nepmucin is localized to the luminal surface as well as the endocytic compartment of LN HEVs, an expression pattern that is compatible with the idea that nepmucin can serve as an HEV-associated cell surface ligand of L-selectin.

Nepmucin can mediate L-selectin–dependent cell rolling through its mucin-like domain

We next investigated whether nepmucin, when appropriately glycosylated, can mediate L-selectin–dependent lymphocyte rolling under physiological shear stress. For this purpose, we first produced a series of nepmucin-Fc chimeric proteins in A5-Core1 cells, which express a specific set of carbohydrate-modifying enzymes (core2 β-1,6-*N*-acetylglucosaminyltransferase [C2GnT] [35], core1 extension-β1,3-*N*-acetylglucosaminyltransferase [C1GnT] [4], FucTVII [5], and LSST [6]), which together generate L-selectin–reactive oligosaccharides. As shown in Fig. 6 A, the nepmucin full-length (FL)-Fc and ΔIg-Fc chimeras as well as GlyCAM-1-Fc bound the MECA-79 mAb, whereas the Δmucin-Fc chimera did not, indicating that the chimeric proteins bearing an intact mucin domain were all appropriately glycosylated.

We next examined whether nepmucin supports lymphocyte rolling under flow conditions using these chimeric proteins. The recombinant proteins were immobilized on the inside wall of glass capillary tubes, and lymphocytes were infused into the capillaries at a shear stress of 0.8 dyne/cm^2 (Fig. 6 B). We found that lymphocytes rolled on the surface when it was coated with nepmucin FL-Fc, ΔIg-Fc, or GlyCAM-1-Fc, but not with Δmucin-Fc, indicating that upon appropriate glycosylation, nepmucin can mediate lymphocyte rolling through its mucin-like domain. As shown in Fig. 6 C, the velocity class with the highest number of rolling cells was 90–100 μm/s (average rolling velocity: 93.6 ± 30.1 μm/s, $n = 70$) on FL-Fc, whereas it was 110–120 μm/s (average rolling velocity: 106.5 ± 21.5 μm/s, $n = 70$) on GlyCAM-1-Fc, indicating that nepmucin can mediate lymphocyte rolling at least as effectively as GlyCAM-1 in vitro. Pretreatment of the lymphocytes with an anti–L-selectin mAb or EDTA (Fig. 6 D), or treatment of the immobilized nepmucin FL-Fc with the MECA-79 mAb, OSGE, or sialydase (Fig. 6 E), completely abrogated the rolling, indicating that the rolling was mediated by lymphocyte L-selectin and the MECA-79 epitope-bearing oligosaccharides on nepmucin. Collectively, these results demonstrate that upon appropriate glycosylation, nepmucin can serve as a functional scaffold for L-selectin–reactive carbohydrates to mediate L-selectin–dependent lymphocyte rolling under physiological flow conditions.

Nepmucin can bind lymphocytes through its Ig domain under static conditions

Nepmucin carries an Ig domain that is linked in tandem to the mucin-like domain in its extracellular region. This structural feature led us to speculate that nepmucin mediates lymphocyte binding through its Ig domain, as is the case with

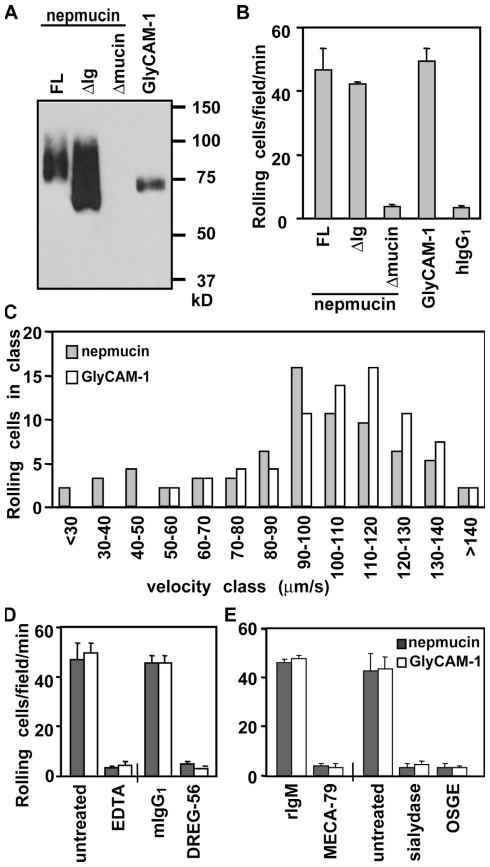

Figure 6. L-selectin–dependent cell rolling mediated by nepmucin-Fc produced in CHO cells expressing C2GnT, C1GnT, FucTVII, and LSST. (A) Preparation of chimeric proteins decorated with MECA-79$^+$ sugar chains. Nepmucin FL-Fc, ΔIg-Fc, Δmucin-Fc, and GlyCAM-1-Fc were produced in the A5-Core1 cells and analyzed with MECA-79 mAb. (B) Lymphocyte rolling on immobilized chimeras under flow. The inside wall of capillary tubes was coated with one of the chimeric proteins or human IgG (20 μg/ml). Jurkat cells (2 × 10^6 cells/ml) were infused into the capillary tubes (0.8 dyne/cm^2), and the rolling cell number was determined. (C) Lymphocyte rolling velocity at a shear stress of 0.8 dyne/cm^2. The histograms display the rolling cell number observed at the indicated rolling velocity. (D) Inhibition of lymphocyte rolling by EDTA or anti–L-selectin mAb. Lymphocytes were pretreated with EDTA, anti–L-selectin (DREG-56), or control human IgG$_1$ before the infusion. (E) Inhibition of lymphocyte rolling by treating immobilized nepmucin with MECA-79, OSGE, or sialydase. Glass capillaries were first coated with Fc chimeras and treated as indicated before the rolling assay.

MAdCAM-1 (19). To test this hypothesis, we performed a lymphocyte-binding assay under static conditions. As shown in Fig. 7 A, immobilized nepmucin FL-Fc or Δmucin-Fc produced in the A5-Core1 cells showed readily detectable binding of unstimulated lymphocytes, whereas nepmucin ΔIg-Fc, GlyCAM-1-Fc, ICAM-1-Fc, or human IgG_1 did not. When the lymphocytes were stimulated with PMA, nepmucin FL-Fc and Δmucin-Fc, but not ΔIg-Fc, showed increased lymphocyte binding, the extent of which was comparable to that observed with ICAM-1-Fc. The lymphocyte binding to nepmucin was apparently independent of L-selectin–reactive sugar chains because nepmucin chimeras prepared in Cos-7 cells, which do not modify proteins with these sugars, gave essentially the same results as described above (unpublished data). When the immobilized nepmucin Δmucin-Fc was treated with a panel of anti-nepmucin mAbs (ZAQ1, ZAQ2, ZAQ3, and ZAQ4) that recognize the Ig domain of nepmucin, ZAQ3 and ZAQ4 abolished the lymphocyte binding, whereas ZAQ1, ZAQ2, and control rat IgG did not. Collectively, these results indicate that nepmucin can bind lymphocytes through its Ig domain and that one or more epitopes in nepmucin's Ig domain are critical for their binding.

We next examined whether the LFA-1 and VLA-4 adhesion pathways are involved in the lymphocyte binding to nepmucin. To this end, lymphocytes were pretreated with neutralizing mAbs to LFA-1 or VLA-4, either alone or in combination, and tested for their binding to nepmucin in the presence or absence of PMA. As shown in Fig. 7 C, the preincubation of lymphocytes with anti–LFA-1 in the presence of PMA abrogated lymphocyte binding to ICAM-1 but not to nepmucin. Similarly, pretreatment with anti–VLA-4 in the presence of PMA abrogated lymphocyte binding to MAdCAM-1 but not to nepmucin. It is of note that lymphocytes bound to nepmucin moderately well in the absence of PMA, and this binding was not affected by anti–LFA-1 or anti–VLA-4. These results indicate that lymphocytes bind to nepmucin independently of the LFA-1 and VLA-4 adhesion pathways.

To further address possible involvement of integrins in lymphocyte binding to nepmucin, we tested divalent cation requirements by using EDTA and Mn^{2+}. As shown in Fig. 7 D, EDTA totally abolished PMA-induced LFA-1–dependent lymphocyte binding to ICAM-1 but only partially to nepmucin. Mn^{2+} significantly increased lymphocyte binding to ICAM-1 but failed to affect that to nepmucin. Shear resistance is a hallmark of integrin-mediated lymphocyte binding

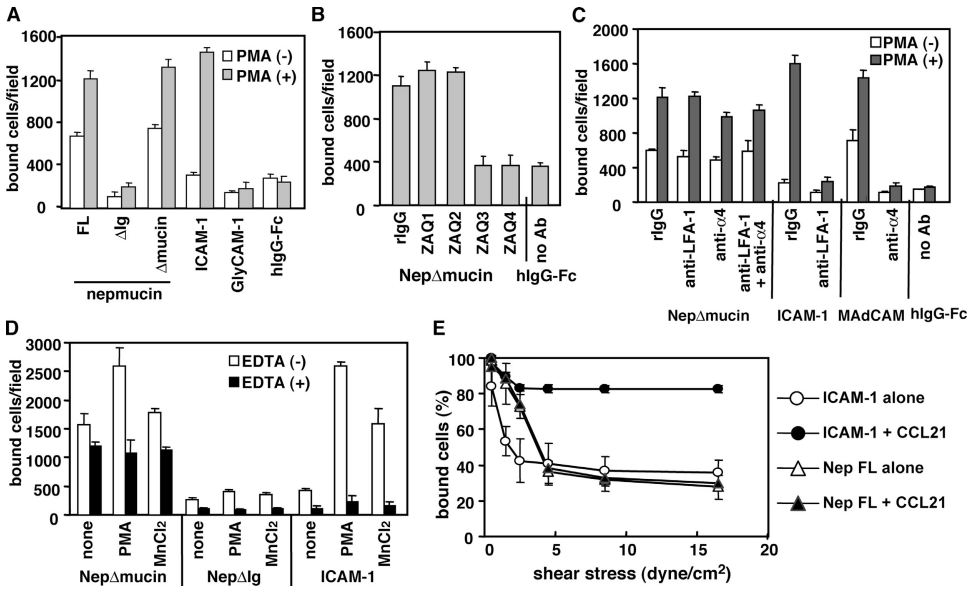

Figure 7. Lymphocyte binding to nepmucin via its Ig domain. (A) Binding of lymphocytes to nepmucin-Fc chimeras. Nepmucin FL-Fc, ΔIg-Fc, Δmucin-Fc, GlyCAM-1-Fc, ICAM-1-Fc, and human IgG_1 Fc were immobilized on glass slides and incubated with splenocytes in the presence or absence of PMA. The number of cells bound per unit area was determined microscopically, and the mean ± SD from three independent areas is given. The data are representative of at least three independent experiments. (B) Effects of anti-nepmucin mAb pretreatment on lymphocyte adhesion. Coated proteins were incubated with a panel of anti-nepmucin mAbs that specifically recognize the Ig domain (ZAQ1, ZAQ2, ZAQ3, and ZAQ4) or with the control rat IgG. The number of cells bound under PMA stimulation is shown. (C) The effects of anti–LFA-1 and/or anti–VLA-4 on nepmucin-mediated lymphocyte binding. Lymphocytes pretreated with anti–LFA-1 and/or anti–VLA-4 or rat IgG were incubated with or without PMA. (D) Effects of EDTA and Mn^{2+} on nepmucin-mediated lymphocyte binding. Splenocytes were preincubated in the presence or absence of EDTA on immobilized proteins and stimulated with or without PMA or $MnCl_2$. (E) Detachment of lymphocytes bound to nepmucin under flow. Fc chimeras were immobilized on the inner surface of glass capillaries with or without CCL21. Lymphocytes were injected into the capillaries and allowed to accumulate on the substrate at a shear stress of 0.125 dyne/cm^2. The shear stress was then increased in twofold increments every 20 s. The lymphocytes that remained adherent at each shear-stress level were counted and expressed as a percentage of the initially bound cells.

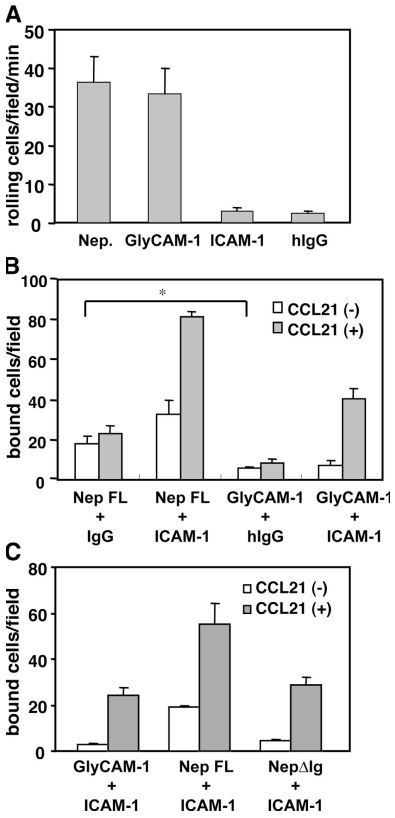

Figure 8. Enhancement of lymphocyte adhesion to an ICAM-1–coated substrate by nepmucin under flow conditions. (A) Lymphocyte rolling on Fc chimeras under flow conditions. Nepmucin FL-Fc, GlyCAM-1-Fc, ICAM-1-Fc, or human IgG was immobilized on the inside wall of capillary tubes that had been coated with goat anti–human IgG. Lymphocytes were infused into the capillary tubes (1.1 dyne/cm^2), and the number of cells that rolled in 0.64 mm^2 per min was counted. (B) Lymphocyte adhesion on nepmucin FL-Fc coimmobilized with ICAM-1-Fc under flow conditions. Fc chimeric proteins were coimmobilized on the inside of capillary tubes with or without CCL21 as indicated. Lymphocytes were infused into the capillary, and the number of bound cells in 0.29 mm^2 was determined. Data represent the mean ± SD from three independent areas. *, $P < 0.005$. (C) Lymphocyte adhesion to nepmucin's Ig domain under flow. Fc chimeras and CCL21 were immobilized on the inside of capillaries as in B. Lymphocytes were injected into the capillaries, and bound cells were counted.

upon chemokine stimulation. As observed in Fig. 7 E, upon lymphocyte stimulation with CCL21, lymphocytes bound to ICAM-1 via integrin LFA-1 in a shear-resistant manner. In sharp contrast, even in the presence of CCL21, lymphocytes bound to nepmucin detached when shear stress was increased (>2.0 dyne/cm^2; Fig. 7 E). Collectively, these observations suggest that lymphocyte binding to nepmucin is independent of lymphocyte integrins.

Nepmucin promotes lymphocyte adhesion in combination with ICAM-1 under flow conditions

We next investigated whether nepmucin cooperates with ICAM-1 to mediate chemokine-driven shear-resistant lymphocyte adhesion under physiological flow conditions. To this end, the nepmucin FL-Fc was immobilized either alone or in combination with ICAM-1-Fc on the inner surface of capillary tubes in the presence or absence of CCL21, and lymphocytes were infused into the capillary at a shear stress of 1.1 dyne/cm^2. GlyCAM-1-Fc and human IgG were used as controls. When immobilized alone, nepmucin FL-Fc and GlyCAM-1-Fc mediated lymphocyte rolling at comparable levels (Fig. 8 A). As shown in Fig. 8 B, in the absence of CCL21, nepmucin FL-Fc but not GlyCAM-1-Fc coimmobilized with either the control IgG or ICAM-1-Fc showed a small but measurable amount of lymphocyte adhesion ($P < 0.005$). When CCL21 was coimmobilized as well, shear-resistant adhesion of rolling lymphocytes was observed in capillaries coated with nepmucin FL-Fc or GlyCAM-1-Fc in combination with ICAM-1-Fc. The number of lymphocytes bound to the capillaries coated with nepmucin FL-Fc plus ICAM-1-Fc (81.7 ± 7.0 cells/field) was about twofold that observed in the capillaries coated with GlyCAM-1-Fc plus ICAM-1-Fc (40.7 ± 4.7 cells/field). The increased lymphocyte binding was not observed with nepmucin that lacks the Ig domain (Fig. 8 C). Collectively, these observations indicate that in combination with ICAM-1, nepmucin can enhance the chemokine-driven shear-resistant adhesion of rolling lymphocytes via its Ig domain under physiological flow conditions.

DISCUSSION

In this study, we identified a novel HEV-associated sialomucin, nepmucin, which is selectively expressed in LN HEVs but not detectable in PP HEVs at the protein level. At least the two higher molecular weight isoforms of peripheral LN HEV-derived nepmucin (75 and 95 kD) are decorated with L-selectin–reactive oligosaccharides bearing the MECA-79 epitope and bind L-selectin. Upon appropriate glycosylation, nepmucin can support L-selectin–dependent lymphocyte rolling under physiological flow conditions in vitro. Furthermore, nepmucin mediates lymphocyte binding via its Ig domain, apparently independently of lymphocyte LFA-1 and VLA-4, and, in combination with ICAM-1, can enhance chemokine-driven shear-resistant lymphocyte binding. Collectively, these observations indicate that nepmucin can serve as a dual-functioning sialomucin, mediating both lymphocyte rolling and binding through its mucin-like domain and Ig domain, respectively.

Previously identified PNAd-forming sialomucins, such as CD34, podocalyxin, and endomucin, are widely expressed in the vascular endothelial cells of a variety of tissues. In contrast, nepmucin was preferentially expressed in the endothelial cells of small blood vessels in various tissues, including capillaries of the heart and spleen, and in LN HEVs, but was not detectable in PP HEVs. Currently, the transcriptional regulation of the nepmucin gene remains unknown.

Alternative splicing of the nepmucin gene generates four splice variants in which the mucin-like domain is of different lengths (isoforms A–D). All are expressed in the LN HEVs. Of these, the two with the higher molecular weight (75 and 95 kD) were decorated with L-selectin–reactive sugar chains

carrying the MECA-79 epitope, which binds L-selectin. PNAd components with an apparent molecular size of ~90 kD have been reported to be comprised of multiple sialomucins (36), including CD34 (11, 12) and endomucin (13, 14). The presence of a PNAd component of 75 kD has also been reported in the mouse LN (17). Thus, the 95- and 75-kD isoforms of nepmucin described here might have been included in the previously detected PNAd components.

The in vitro rolling experiments clearly showed that recombinant nepmucin, which was produced in A5-Core1 cells expressing a specific set of carbohydrate-modifying enzymes (C2GnT, C1GnT, FucTVII, and LSST), supported lymphocyte rolling under physiological flow conditions that was abolished by the anti–L-selectin or MECA-79 mAb, indicating that appropriately glycosylated nepmucin can mediate L-selectin–dependent lymphocyte rolling. The nepmucin's mucin-like domain was necessary for this activity because nepmucin mutants lacking the mucin-like domain but not the Ig domain failed to support lymphocyte rolling. The lymphocyte rolling behavior observed on the nepmucin chimera was quantitatively and qualitatively comparable to that observed on the GlyCAM-1 chimeric protein. Nepmucin was distributed to the microvillous structure on the luminal surface of LN HEVs where L-selectin ligands are localized (33). These observations fully support the hypothesis that nepmucin serves as a functional ligand for L-selectin and mediates lymphocyte rolling when appropriately glycosylated by a specific set of carbohydrate-modifying enzymes in LN HEVs.

Multiple sialomucins contribute to the generation of functional PNAd in LN HEVs. It remains unclear, however, whether different PNAd components expressed in LN HEVs play either distinct or redundant roles in lymphocyte rolling. The absence of overt defects in lymphocyte trafficking across the HEV walls in mice deficient in CD34 (36), GlyCAM-1, or both (37) supports the hypothesis that the HEV-associated sialomucins cooperate functionally to play redundant roles so that the loss of one or more PNAd member can be compensated for by other members. We are now attempting to inactivate the nepmucin gene in vivo so that we can directly assess nepmucin's role in HEVs.

The trafficking of lymphocytes to the LNs and PPs is initiated by lymphocyte rolling on HEVs, which is followed by firm adhesion of lymphocytes to the luminal surface of HEVs. Although the mucosal addressin MAdCAM-1 in PP HEVs has been shown to participate in both lymphocyte rolling on (18) and adhesion to (19) PP HEVs, the PNAd components in LN HEVs have been thought to play a role only in the initial lymphocyte rolling process, but not in the subsequent lymphocyte adhesion step. In this regard, we note that unlike most conventional sialomucins expressed in LN HEVs, nepmucin carries an NH_2-terminal Ig domain and supports lymphocyte binding via the Ig domain in the apparent absence of the lymphocyte integrins LFA-1 and VLA-4 under static conditions. Furthermore, in combination with ICAM-1, nepmucin enhanced CCL21-driven shear-resistant lymphocyte adhesion, suggesting that nepmucin contributes to the step of the adhesion of lymphocytes to HEVs. Nepmucin may decelerate the velocity of rolling lymphocytes through its Ig domain and thereby successfully bridge the initial rolling and subsequent adhesion steps of lymphocytes in the HEVs, as has been suggested for MAdCAM-1 (38). The identification of putative counterreceptor(s) for nepmucin's Ig domain should help elucidate this issue.

The Ig domain of nepmucin has substantial homology to that of the mouse polymeric Ig receptor (28) and CMRF-35 family members (human CMRF-35A [25], CMRF-35H [26], and mouse DIgR [27]). Recently, Chung et al. (30) found that a gene cluster of the mouse CMRF-35–like molecule (CLM) family (CLM-1-9) is located on chromosome 11. They changed the name of mouse DIgR to CLM-4 and suggested that mouse CLM-5 and CLM-8 are the human homologues of CMRF-35A and CMRF-35H, respectively. Based on the sequence identity, nepmucin appears to correspond to CLM-9. Because *CLM-9* lies apart from the genes encoding the other CLM members, which are all clustered within 240 kb on chromosome 11, nepmucin/CLM-9 may be a distant relative of the other CLM family members. The gene encoding the human ortholog of nepmucin was found in the GenBank database (accession no. BC025395). Like mouse nepmucin, the human counterpart bears a potential protein kinase C phosphorylation site and a cluster of negative charges in its cytoplasmic region, suggesting that nepmucin and its human ortholog participate in intracellular signaling.

In conclusion, our study demonstrates that a novel LN HEV-associated sialomucin, nepmucin, mediates lymphocyte rolling and binding through its mucin-like domain and Ig domain, respectively. Further investigation of the physiological significance of nepmucin in vivo is now warranted, which should lead to a more precise understanding of the molecular mechanisms underlying homeostatic lymphocyte trafficking across the HEVs.

MATERIALS AND METHODS

Animals. C57BL/6 mice were purchased from CLEA Japan and Japan SLC. SD rats were purchased from CLEA Japan. The experimental protocol was approved by the Ethics Review Committee for Animal Experimentation of Osaka University Medical School.

Reagents. Biotinylated mAbs to mouse B220 (RA3-6B2), CD3 (145-2C11), CD11c (HL3), and CD31 (MEC13.3) were obtained from BD Biosciences. The hybridomas producing anti-PNAd mAb (MECA-79) and anti–MAdCAM-1 mAb (MECA-367) were provided by E.C. Butcher (Stanford University School of Medicine, Stanford, CA) (8, 39). The mouse L-selectin-IgG chimeric protein (LEC/IgG) was produced in COS-7 cells as described previously (40).

Full-length cDNA library of PNAd$^+$ HEVs. PNAd$^+$ HEV cells were purified as described previously (23), and total RNA was isolated with TRIzol reagent (Invitrogen). A cDNA library was prepared using a SMART cDNA library construction kit (CLONTECH Laboratories, Inc.). The original PNAd$^+$ HEV cDNA library contained 6.5×10^6 recombinants/ml before amplification.

Isolation of nepmucin cDNA. By comparing the expression profiles of PNAd$^+$ HEVs with those of 38 other tissue and cell types (23, 24), we

identified a 3′-cDNA fragment of nepmucin (GS11753). A corresponding cDNA sequence was found in the GenBank EST database (AK009375). To isolate full-length nepmucin cDNA, a cDNA fragment was amplified by PCR using a primer pair (sense, 5′-CAAGAGCTCTCGATGACCGTG-3′; antisense, 5′-TCTCCTCCAGCAATTGATGCAG-3′) alkaline phosphatase labeled by AlkPhos Direct (GE Healthcare) and used for screening the PNAd$^+$ HEV cDNA library by plaque hybridization. Duplicate filter lifts containing 5.0×10^4 plaques were hybridized at 55°C overnight, and 30 independent clones were obtained and sequenced. Comparison with the genomic sequence (AL591145) showed these clones represented four splicing isoforms (isoforms A–D; see Fig. 1 B).

RT-PCR. Total RNA was extracted using TRIzol reagent (Invitrogen) from purified PNAd$^+$ HEVs, MAdCAM-1$^+$ HEVs, endothelial cell lines (KOP2.16, SVEC4-10, bEND3, and F2), monocyte/macrophage cell lines (WEHI3B, MH-S, and P388D1), a mast cell line (P815), freshly isolated CD3$^+$ T cells, B220$^+$ B cells, and CD11c$^+$ DCs from peripheral LNs purified by autoMACS (Miltenyi Biotec). Single-strand cDNA was synthesized using the Ready-To-Go kit (GE Healthcare) and used in RT-PCR with Ex-Taq DNA polymerase (Takara Bio). PCR was performed at 95°C for 5 min, 32 cycles at 94°C for 30 s, at 62°C for 30 s, at 72°C for 1 min, and a final extension at 72°C for 5 min using the following primer pairs: β-actin: sense, 5′-ATGGATGACGATATCGCT-3′, antisense, 5′-ATGAGGTAGTCTGTCAGGT-3′; and nepmucin: sense, 5′-AGACTCGACGATAGACCTTGCAG-3′, antisense, 5′-TCTCCTCCAGCAATTGATGCAG-3′, all the nepmucin isoforms detected as a single band; sense, 5′-CAAGAGCTCTCGATGACCGTG-3′, antisense, 5′-CACAGAGATGAACTCAGAGAAGG-3′, the nepmucin splicing isoforms detected as distinct bands with different product sizes.

Generation of nepmucin-human Ig chimeras. cDNA fragments encoding the extracellular domain of full-length nepmucin (isoform A, amino acids 19–284), nepmucin lacking the mucin-like domain (isoform D, amino acids 19–126 connected to 255–284), and nepmucin lacking the Ig domain (amino acids 126–284) were amplified by PCR and inserted into the CD5 leader hIgG vector (provided by B. Seed, Harvard Medical School, Boston, MA). COS-7 cells were transfected with the plasmids by a DEAE-dextran method, and the chimeric proteins (termed FL-Fc, Δmucin-Fc, and ΔIg-Fc, respectively) were purified from the culture supernatant with Hitrap protein A (GE Healthcare).

Generation of mAbs against nepmucin. The protein A–purified chimeric protein (FL-Fc) was injected into the footpads of female SD rats, and the popliteal LN cells were fused with P3-X63.Ag8.653 mouse myeloma cells. Hybridomas producing anti-nepmucin mAb (ZAQ1, ZAQ2, ZAQ3, ZAQ4, and ZAQ5 [all IgG2a]) were cloned by limiting dilution. These ZAQ antibodies recognized the Ig domain of nepmucin, as determined by ELISA using nepmucin-Fc chimeras.

Western blotting and immunoprecipitation. Mouse tissue lysates were prepared as described previously (14). For Western blot analyses, samples from each tissue (30 μg/lane) were separated by SDS-PAGE under nonreducing conditions and transferred to PVDF filters. After being blocked with PBS containing 3% BSA, the filter was incubated with an anti-nepmucin mAb (ZAQ2) or control rat IgG2a (Santa Cruz Biotechnology, Inc.), followed by horseradish peroxidase–conjugated goat anti–rat IgG (American Qualex). For immunoprecipitation, the peripheral LN lysate was precleared with protein G–sepharose 4B (GE Healthcare), and $CaCl_2$ was added to restore the calcium ion concentration (2 mM). The anti-nepmucin mAb ZAQ2 or LEC/IgG premixed with protein G–sepharose 4B was added to the lysate, and the solution was incubated at 4°C overnight. The precipitated materials were subjected to SDS-PAGE and immunoblotting using a combination of MECA-79 mAb and horseradish peroxidase anti–rat IgM (Jackson ImmunoResearch Laboratories) or biotinylated anti-nepmucin (ZAQ2) and ABC reagent (Vector Laboratories). For reimmunoprecipitation experiments, LN lysates were first precipitated with LEC/IgG, eluted with 5 mM EDTA, and subjected to reprecipitation with anti-nepmucin (ZAQ2) or control rat IgG. The precipitated proteins were analyzed by Western blotting using the MECA-79 mAb. Biotinylated rat IgG2a (anti-CD8α [53–6.7]; eBioscience) and rat IgM (Chemicon International) were used as isotype-matched controls for ZAQ2 and MECA-79, respectively.

Enzyme treatment of nepmucin. For *O*-deglycosylation, nepmucin affinity purified from heart lysates was treated with a mixture of 50 mU/ml α-1,3/4-L-fucosidase (Takara Bio), 0.16 U/ml sialydase from *Clostridium perfingen* (Prozyme), 0.1 U/ml β-1,4-galactosidase (Prozyme), 2 U/ml β-*N*-acetylglucosaminidase (Prozyme), and 40 mU/ml endo-α-*N*-acetylgalactosaminidase (*O*-glycanase; Glyko) in 50 mM sodium phosphate, pH 7.0, at 37°C for 40 h. The samples were subjected to SDS-PAGE and Western blotting using biotinylated anti-nepmucin (ZAQ3) and ABC reagent. For OSGE digestion, L-selectin–binding materials from peripheral LNs were treated with 0.3 mg/ml OSGE (Cedarlane) in PBS at 37°C overnight and subjected to reprecipitation with an anti-nepmucin (ZAQ2). For sialydase digestion, the L-selectin–binding materials were reprecipitated with an anti-nepmucin mAb, ZAQ2, followed by incubation with 0.2 U/ml sialydase in 50 mM sodium phosphate, pH 5.5, at 37°C overnight. These samples were analyzed by Western blotting using the MECA-79 mAb.

Immunohistochemistry. Frozen sections were fixed in acetone, blocked with Block Ace (Dainippon Seiyaku), and incubated with an anti-nepmucin mAb (ZAQ1 or ZAQ2) or control rat IgG (Cappel), followed by FITC-conjugated goat anti–rat IgG (Cappel). After blocking with rat IgG, the sections were further incubated with a combination of biotinylated mAbs (MECA-79, MECA-367, or MEC13.3 [anti-CD31]) and Alexa Fluor 594–conjugated streptavidin (Invitrogen).

Immunoelectron microscopy. Immunoelectron microscopy was performed as described previously (41). In brief, mice were fixed by transcardial perfusion of cold periodate-lysine-paraformaldehyde solution, and the peripheral LNs were removed. After postfixation with the same fixative, the samples were embedded in OCT compound (Sakura) and snap frozen. 10-μm-thick frozen sections were incubated with the culture supernatant of an anti-nepmucin mAb, ZAQ5, followed by ABC reagent. The sections were then fixed with 1% glutaraldehyde and 2% osmium tetroxide solutions, dehydrated in graded ethanol, and embedded in epoxy resin. Ultrathin sections were stained with lead citrate and examined in a transmission electron microscope (JEM-1230; JEOL).

Generation of recombinant nepmucin-Fc carrying MECA-79 epitopes. CHO cells stably expressing human C2GnT, human FucTVII (42), and human LSST (6) (A5 cells) (14) were transfected with pcDNA6 (Invitrogen) containing a cDNA encoding human C1GnT (4). The resulting line was called A5-Core1 cells. The A5-Core1 cells were transiently transfected with expression plasmids containing cDNA encoding FL-Fc, Δmucin-Fc, ΔIg-Fc, or GlyCAM-1-Fc (6) using the Escort V lipofection reagent (Sigma-Aldrich). Chimeric proteins were purified from the culture supernatant using a protein A column.

Rolling assay. The inside wall of 0.69-mm-diameter capillary tubes (Drummond Scientific) was coated with one of the recombinant proteins (20 μg/ml) in Tris-buffered saline, pH 9.0, at 4°C overnight and blocked with FCS for 5 min at room temperature. Jurkat cells (2×10^6 cells/ml) were infused into the capillary at a shear stress of 0.8 dyne/cm^2 at room temperature. The flow rate was controlled by a Harvard syringe pump (PHD 2000; Instech Laboratories). 3 min after the start of the infusion, cell images were recorded with a cell-viewing system (SRM-100; Nikon) and video recorder (BR-S600; Victor). For the inhibition studies, the cells were pretreated with 5 μg/ml anti–L-selectin (DREG-56; BD Biosciences) or 10 mM EDTA. In some experiments, the immobilized proteins were pretreated with 5 μg/ml

MECA-79, 50 mU/ml sialydase in 50 mM sodium acetate, pH 5.2, containing 0.1% BSA, or 0.16 mg/ml of OSGE in PBS, or left untreated.

Static adhesion assay. 4-mm-diameter multiwell glass slides were coated with 10 μg/ml recombinant nepmucin-Fc, GlyCAM-1-Fc, rat ICAM-1-Fc (provided by Y. Iigo, Daiichi Pharmaceutical Co., Tokyo, Japan), rat MAdCAM-1-Fc (43), or recombinant human IgG_1 Fc (R&D Systems) at 4°C overnight and blocked with FCS. 2×10^5 plastic nonadherent spleen cells were added and allowed to settle for 5 min. PMA (50 ng/ml final concentration) or control buffer (RPMI 1640 containing 0.1% BSA) was added, and the cells were incubated for an additional 5 min at 37°C. After the unbound cells were washed off, the bound cells were counted. For blocking experiments, immobilized chimeric proteins were preincubated with anti-nepmucin mAbs or rat IgG for 45 min, or splenocytes were preincubated with anti-CD11a (KBA) (44) or anti-CD49d (PS/2) (45) (20 μg/ml) for 10 min. In some experiments, splenocytes were incubated on the chimeric protein–coated slide glass in the presence or absence of 10 mM EDTA, followed by an additional incubation for 5 min with or without 50 ng/ml PMA or 2 mM $MnCl_2$.

Detachment assay. The inside wall of glass capillaries was coated with nepmucin FL-Fc or ICAM-1-Fc (10 μg/ml each) at 4°C overnight and blocked with FCS for 5 min. The downstream half of each tube was additionally coated with 2 μM mouse CCL21 (R&D Systems). Plastic nonadherent spleen cells (10^6 cells/ml) were injected into the capillary tubes at 0.125 dyne/cm^2 for 5 min at 37°C. The flow was then increased in twofold increments every 20 s. The number of the cells that remained bound in an 0.18-mm^2 microscope field was determined by counting at each interval.

Flow adhesion assay. The inner surface of glass capillary tubes was coated with 10 μg/ml goat anti–human IgG (Cappel), followed by nepmucin-Fc or GlyCAM-1-Fc in combination with ICAM-1-Fc or human IgG (20 μg/ml each) for 2 h at room temperature, and blocked with FCS for 5 min. Additionally, the downstream half of each tube was coated with 2 μM mouse CCL21 for 5 min. Mouse splenocytes were prepared as described previously (46), and the cells (3×10^6 cells/ml) were infused into the capillaries at a shear stress of 1.1 dyne/cm^2 at 37°C. After a 1–2-min stabilization period, the cell behavior was monitored as described above. The number of cells bound (i.e., that remained stationary for at least 20 s) per randomly selected 0.29-mm^2 microscope field was determined 9 min after the start of monitoring.

Statistical analysis. A Student's *t* test was applied to compare the statistical difference within two groups.

Online supplemental material. Fig. S1 shows results obtained in in situ hybridization and real-time PCR analyses for nepmucin expression in HEVs of mesenteric LNs and PPs. Fig. S1 and supplemental Materials and methods are available at http://www.jem.org/cgi/content/full/jem.20052543/DC1.

We thank Dr. E.C. Butcher for the MECA-79 and MECA-367 mAbs, B. Seed for the CD5 leader hIgG vector, Y. Iigo for the rat ICAM-1-Fc, and Dr. S. Uematsu for technical advice on real-time PCR. We thank H. Hayasaka for helpful comments on the manuscript. We also thank T. Kondo for technical support as well as S. Yamashita and M. Komine for secretarial assistance.

This work was supported in part by Grants-in-Aid 17047025 (to T. Tanaka), 17046010 (to T. Tanaka), 17590432 (to T. Tanaka), and 17014056 (to M. Miyasaka) from the Ministry of Education, Culture, Sports, Science and Technology of Japan and by National Institutes of Health grants CA48737 and PO1 CA71932 (both to M. Fukuda).

The authors have no conflicting financial interests.

Submitted: 22 December 2005
Accepted: 10 May 2006

REFERENCES

1. von Andrian, U.H., and T.R. Mempel. 2003. Homing and cellular traffic in lymph nodes. *Nat. Rev. Immunol.* 3:867–878.
2. Miyasaka, M., and T. Tanaka. 2004. Lymphocyte trafficking across high endothelial venules: dogmas and enigmas. *Nat. Rev. Immunol.* 4:360–370.
3. Rosen, S.D. 2004. Ligands for L-selectin: homing, inflammation, and beyond. *Annu. Rev. Immunol.* 22:129–156.
4. Yeh, J.C., N. Hiraoka, B. Petryniak, J. Nakayama, L.G. Ellies, D. Rabuka, O. Hindsgaul, J.D. Marth, J.B. Lowe, and M. Fukuda. 2001. Novel sulfated lymphocyte homing receptors and their control by a Core1 extension β1,3-*N*-acetylglucosaminyltransferase. *Cell.* 105:957–969.
5. Maly, P., A. Thall, B. Petryniak, C.E. Rogers, P.L. Smith, R.M. Marks, R.J. Kelly, K.M. Gersten, G. Cheng, T.L. Saunders, et al. 1996. The α(1,3)fucosyltransferase Fuc-TVII controls leukocyte trafficking through an essential role in L-, E-, and P-selectin ligand biosynthesis. *Cell.* 86:643–653.
6. Hiraoka, N., B. Petryniak, J. Nakayama, S. Tsuboi, M. Suzuki, J.C. Yeh, D. Izawa, T. Tanaka, M. Miyasaka, J.B. Lowe, and M. Fukuda. 1999. A novel, high endothelial venule-specific sulfotransferase expresses 6-sulfo sialyl Lewis(x), an L-selectin ligand displayed by CD34. *Immunity.* 11:79–89.
7. Hemmerich, S., A. Bistrup, M.S. Singer, A. van Zante, J.K. Lee, D. Tsay, M. Peters, J.L. Carminati, T.J. Brennan, K. Carver-Moore, et al.2001. Sulfation of L-selectin ligands by an HEV-restricted sulfotransferase regulates lymphocyte homing to lymph nodes. *Immunity.* 15:237–247.
8. Streeter, P.R., B.T. Rouse, and E.C. Butcher. 1988. Immunohistologic and functional characterization of a vascular addressin involved in lymphocyte homing into peripheral lymph nodes. *J. Cell Biol.* 107:1853–1862.
9. von Andrian, U.H. 1996. Intravital microscopy of the peripheral lymph node microcirculation in mice. *Microcirculation.* 3:287–300.
10. Lasky, L.A., M.S. Singer, D. Dowbenko, Y. Imai, W.J. Henzel, C. Grimley, C. Fennie, N. Gillett, S.R. Watson, and S.D. Rosen. 1992. An endothelial ligand for L-selectin is a novel mucin-like molecule. *Cell.* 69:927–938.
11. Baumhueter, S., M.S. Singer, W. Henzel, S. Hemmerich, M. Renz, S.D. Rosen, and L.A. Lasky. 1993. Binding of L-selectin to the vascular sialomucin CD34. *Science.* 262:436–438.
12. Puri, K.D., E.B. Finger, G. Gaudernack, and T.A. Springer. 1995. Sialomucin CD34 is the major L-selectin ligand in human tonsil high endothelial venules. *J. Cell Biol.* 131:261–270.
13. Samulowitz, U., A. Kuhn, G. Brachtendorf, R. Nawroth, A. Braun, A. Bankfalvi, W. Bocker, and D. Vestweber. 2002. Human endomucin: distribution pattern, expression on high endothelial venules, and decoration with the MECA-79 epitope. *Am. J. Pathol.* 160:1669–1681.
14. Kanda, H., T. Tanaka, M. Matsumoto, E. Umemoto, Y. Ebisuno, M. Kinoshita, M. Noda, R. Kannagi, T. Hirata, T. Murai, et al. 2004. Endomucin, a sialomucin expressed in high endothelial venules, supports L-selectin-mediated rolling. *Int. Immunol.* 16:1265–1274.
15. Sassetti, C., K. Tangemann, M.S. Singer, D.B. Kershaw, and S.D. Rosen. 1998. Identification of podocalyxin-like protein as a high endothelial venule ligand for L-selectin: parallels to CD34. *J. Exp. Med.* 187:1965–1975.
16. Hemmerich, S., E.C. Butcher, and S.D. Rosen. 1994. Sulfation-dependent recognition of high endothelial venules (HEV)-ligands by L-selectin and MECA 79, and adhesion-blocking monoclonal antibody. *J. Exp. Med.* 180:2219–2226.
17. Berg, E.L., L.M. McEvoy, C. Berlin, R.F. Bargatze, and E.C. Butcher. 1993. L-selectin-mediated lymphocyte rolling on MAdCAM-1. *Nature.* 366:695–698.
18. Berlin, C., R.F. Bargatze, J.J. Campbell, U.H. von Andrian, M.C. Szabo, S.R. Hasslen, R.D. Nelson, E.L. Berg, S.L. Erlandsen, and E.C. Butcher. 1995. α4 integrins mediate lymphocyte attachment and rolling under physiologic flow. *Cell.* 80:413–422.
19. Berlin, C., E.L. Berg, M.J. Briskin, D.P. Andrew, P.J. Kilshaw, B. Holzmann, I.L. Weissman, A. Hamann, and E.C. Butcher. 1993. α4β7 integrin mediates lymphocyte binding to the mucosal vascular addressin MAdCAM-1. *Cell.* 74:185–195.
20. Briskin, M.J., L.M. McEvoy, and E.C. Butcher. 1993. MAdCAM-1 has homology to immunoglobulin and mucin-like adhesion receptors and to IgA1. *Nature.* 363:461–464.
21. Shyjan, A.M., M. Bertagnolli, C.J. Kenney, and M.J. Briskin. 1996. Human mucosal addressin cell adhesion molecule-1 (MAdCAM-1)

demonstrates structural and functional similarities to the α4β7-integrin binding domains of murine MAdCAM-1, but extreme divergence of mucin-like sequences. *J. Immunol.* 156:2851–2857.
22. Briskin, M.J., L. Rott, and E.C. Butcher. 1996. Structural requirements for mucosal vascular addressin binding to its lymphocyte receptor α4β7. Common themes among integrin-Ig family interactions. *J. Immunol.* 156:719–726.
23. Izawa, D., T. Tanaka, K. Saito, H. Ogihara, T. Usui, S. Kawamoto, K. Matsubara, K. Okubo, and M. Miyasaka. 1999. Expression profile of active genes in mouse lymph node high endothelial cells. *Int. Immunol.* 11:1989–1998.
24. Saito, K., T. Tanaka, H. Kanda, Y. Ebisuno, D. Izawa, S. Kawamoto, K. Okubo, and M. Miyasaka. 2002. Gene expression profiling of mucosal addressin cell adhesion molecule-1+ high endothelial venule cells (HEV) and identification of a leucine-rich HEV glycoprotein as a HEV marker. *J. Immunol.* 168:1050–1059.
25. Jackson, D.G., D.N. Hart, G. Starling, and J.I. Bell. 1992. Molecular cloning of a novel member of the immunoglobulin gene superfamily homologous to the polymeric immunoglobulin receptor. *Eur. J. Immunol.* 22:1157–1163.
26. Green, B.J., G.J. Clark, and D.N. Hart. 1998. The CMRF-35 mAb recognizes a second leukocyte membrane molecule with a domain similar to the poly Ig receptor. *Int. Immunol.* 10:891–899.
27. Luo, K., W. Zhang, L. Sui, N. Li, M. Zhang, X. Ma, L. Zhang, and X. Cao. 2001. DIgR1, a novel membrane receptor of the immunoglobulin gene superfamily, is preferentially expressed by antigen-presenting cells. *Biochem. Biophys. Res. Commun.* 287:35–41.
28. Piskurich, J.F., M.H. Blanchard, K.R. Youngman, J.A. France, and C.S. Kaetzel. 1995. Molecular cloning of the mouse polymeric Ig receptor. Functional regions of the molecule are conserved among five mammalian species. *J. Immunol.* 154:1735–1747.
29. Hanisch, F.G., and S. Muller. 2000. MUC1: the polymorphic appearance of a human mucin. *Glycobiology.* 10:439–449.
30. Chung, D.H., M.B. Humphrey, M.C. Nakamura, D.G. Ginzinger, W.E. Seaman, and M.R. Daws. 2003. CMRF-35-like molecule-1, a novel mouse myeloid receptor, can inhibit osteoclast formation. *J. Immunol.* 171:6541–6548.
31. Kraal, G., K. Schornagel, P.R. Streeter, B. Holzmann, and E.C. Butcher. 1995. Expression of the mucosal vascular addressin, MAdCAM-1, on sinus-lining cells in the spleen. *Am. J. Pathol.* 147:763–771.
32. Sutherland, D.R., K.M. Abdullah, P. Cyopick, and A. Mellors. 1992. Cleavage of the cell-surface O-sialoglycoproteins CD34, CD43, CD44, and CD45 by a novel glycoprotease from Pasteurella haemolytica. *J. Immunol.* 148:1458–1464.
33. Kikuta, A., and S.D. Rosen. 1994. Localization of ligands for L-selectin in mouse peripheral lymph node high endothelial cells by colloidal gold conjugates. *Blood.* 84:3766–3775.
34. Mukherjee, S., R.N. Ghosh, and F.R. Maxfield. 1997. Endocytosis. *Physiol. Rev.* 77:759–803.
35. Bierhuizen, M.F., and M. Fukuda. 1992. Expression cloning of a cDNA encoding UDP-GlcNAc:Gal β1-3-GalNAc-R (GlcNAc to GalNAc) β1-6GlcNAc transferase by gene transfer into CHO cells expressing polyoma large tumor antigen. *Proc. Natl. Acad. Sci. USA.* 89:9326–9330.
36. Suzuki, A., D.P. Andrew, J.A. Gonzalo, M. Fukumoto, J. Spellberg, M. Hashiyama, H. Takimoto, N. Gerwin, I. Webb, G. Molineux, et al. 1996. CD34-deficient mice have reduced eosinophil accumulation after allergen exposure and show a novel crossreactive 90-kD protein. *Blood.* 87:3550–3562.
37. Kansas, G.S. 1996. Selectins and their ligands: current concepts and controversies. *Blood.* 88:3259–3287.
38. Bargatze, R.F., M.A. Jutila, and E.C. Butcher. 1995. Distinct roles of L-selectin and integrins α4β7 and LFA-1 in lymphocyte homing to Peyer's patch-HEV in situ: the multistep model confirmed and refined. *Immunity.* 3:99–108.
39. Streeter, P.R., E.L. Berg, B.T. Rouse, R.F. Bargatze, and E.C. Butcher. 1988. A tissue-specific endothelial cell molecule involved in lymphocyte homing. *Nature.* 331:41–46.
40. Hirata, T., G. Merrill-Skoloff, M. Aab, J. Yang, B.C. Furie, and B. Furie. 2000. P-Selectin glycoprotein ligand 1 (PSGL-1) is a physiological ligand for E-selectin in mediating T helper 1 lymphocyte migration. *J. Exp. Med.* 192:1669–1676.
41. Tohya, K., and M. Kimura. 1998. Ultrastructural evidence of distinctive behavior of L-selectin and LFA-1 (αLβ2 integrin) on lymphocytes adhering to the endothelial surface of high endothelial venules in peripheral lymph nodes. *Histochem. Cell Biol.* 110:407–416.
42. Homeister, J.W., A.D. Thall, B. Petryniak, P. Maly, C.E. Rogers, P.L. Smith, R.J. Kelly, K.M. Gersten, S.W. Askari, G. Cheng, et al. 2001. The α(1,3)fucosyltransferases FucT-IV and FucT-VII exert collaborative control over selectin-dependent leukocyte recruitment and lymphocyte homing. *Immunity.* 15:115–126.
43. Iizuka, T., T. Tanaka, M. Suematsu, S. Miura, T. Watanabe, R. Koike, Y. Ishimura, H. Ishii, N. Miyasaka, and M. Miyasaka. 2000. Stage-specific expression of mucosal addressin cell adhesion molecule-1 during embryogenesis in rats. *J. Immunol.* 164:2463–2471.
44. Nishimura, T., and T. Itoh. 1988. Higher level expression of lymphocyte function-associated antigen-1 (LFA-1) on in vivo natural killer cells. *Eur. J. Immunol.* 18:2077–2080.
45. Miyake, K., I.L. Weissman, J.S. Greenberger, and P.W. Kincade. 1991. Evidence for a role of the integrin VLA-4 in lympho-hemopoiesis. *J. Exp. Med.* 173:599–607.
46. Wang, W.C., L.M. Goldman, D.M. Schleider, M.M. Appenheimer, J.R. Subjeck, E.A. Repasky, and S.S. Evans. 1998. Fever-range hyperthermia enhances L-selectin-dependent adhesion of lymphocytes to vascular endothelium. *J. Immunol.* 160:961–969.